



# Paeoniflorin, a constituent of Kami-shoyo-san, suppresses blood glucose levels in postmenopausal diabetic mice by promoting the secretion of estradiol from adipocytes

Kyoko Kobayashi<sup>\*</sup>, Yu Ting Tang, Kenroh Sasaki

Department of Pharmacognosy, Faculty of Pharmaceutical Sciences, Tohoku Medical and Pharmaceutical University, Sendai, Miyagi, 981-8558, Japan

## ARTICLE INFO

### Keywords:

Kami-shoyo-san  
Paeoniflorin  
Estradiol  
Blood glucose level  
Adipocyte  
Ovarian dysfunction

## ABSTRACT

Ovarian functional deterioration in women with climacteric disorders increases the prevalence of type 2 diabetes (T2D). Therefore, we revealed that paeoniflorin (PF), an ingredient of paeony root (PR), which is a constituent of Kami-shoyo-san (KS), promotes glucose uptake by increasing estradiol secretion from adipocytes. Adipocytes differentiated from 3T3-L1 cells were incubated in culture medium containing the extracts of KS, PR, KS excluding PR (KS-PR), or PF for 5 d at 37 °C and 5% CO<sub>2</sub>. The estradiol and glucose concentrations in the medium were determined using enzyme-linked immunosorbent assay (ELISA). Next, PF (1 or 10 mg/kg) was subcutaneously injected into ovariectomized mice (12-week-old, ICR strain) once daily for 19 d to perform the glucose tolerance test and determine blood estradiol and adiponectin levels. The release of estradiol from 3T3-L1 adipocytes was significantly increased by KS, PR, KS-PR, and PF, and the increased estradiol level caused by KS was significantly decreased by excluding PF from KS (KS-PR). Glucose concentration in the medium was significantly decreased by KS and PF. In *in vivo* experiments, the 10 mg/kg PF-treated group showed significantly suppressed blood glucose levels at 0 and 30 min after D-glucose loading by intraperitoneal injection. These findings indicate that KS, which includes PR-containing PF as the main ingredient, may have the potential to prevent T2D caused by ovarian dysfunction in menopausal women by increasing estradiol secretion from adipocytes.

## 1. Introduction

Ovarian functional deterioration in female climacteric disorders increases the prevalence of type 2 diabetes (T2D) [1]. In a large randomized controlled trial, postmenopausal women who were actively treated with estrogen showed significantly ameliorated insulin resistance compared to the placebo group [2]. The cause of T2D in female climacteric disorder is considered to be a decrease in estrogen rebound to half of the original level, accompanied by a marked increase in follicle-stimulating hormone (FSH), leading to an increase in lipid accumulation in adipocytes [3]. These reports suggest a relationship between estrogen levels and glucose metabolism. In this regard, it has been reported that 3T3-L1 adipocytes treated with estradiol show an increase in glucose uptake [4] and ovariectomized mice treated with estradiol exhibit improved insulin resistance [5].

Estradiol bound to estrogen receptor 1 (ESR1) promotes the phosphorylation of serine/threonine-protein kinase (AKT) in the insulin

receptor signaling pathway, leading to the translocation of glucose transporter 4 (GLUT4) to the cell membrane. ESR1 also increases the expression of GLUT4 (gene name: *Scl2a4*) and accelerates glucose uptake in skeletal muscle cells, hepatocytes, and adipocytes [6]. Therefore, the ovarian hormone estradiol plays an important role in glucose uptake and ovarian failure increases the risk of developing diabetes.

Estradiol influences cytokine secretion from mature adipocytes, such as adiponectin, leptin, tumor necrosis factor (TNF)  $\alpha$ , and resistin. Adiponectin secretion is inversely correlated with estradiol secretion, which influences adipogenesis [7]. Adipose tissue is known as a steroidogenesis site for sex hormones such as androgens (testosterone and androstenedione) and estrogens (estrone and estradiol). Mouse embryonic fibroblast 3T3-L1 cells can differentiate into adipocyte-like cells, which can also generate aromatase, catalyzing the biosynthesis pathway for estrogens from androgens [8]. Adipose tissue plays an important role in estradiol synthesis as a substitute for the ovary in climacteric disorders.

Similarly, the  $\gamma$  isoform of peroxisome proliferator-activated receptor

<sup>\*</sup> Corresponding author. Department of Pharmacognosy, Faculty of Pharmaceutical Sciences, Tohoku Medical and Pharmaceutical University, 4-1 Komatsushima 4-Chome, Aoba-Ku, Sendai, Miyagi, 981-8558, Japan.

E-mail address: [k-kyoko@tohoku-mpu.ac.jp](mailto:k-kyoko@tohoku-mpu.ac.jp) (K. Kobayashi).

<https://doi.org/10.1016/j.bbrep.2022.101335>

Received 15 July 2022; Received in revised form 19 August 2022; Accepted 22 August 2022

Available online 5 September 2022

2405-5808/© 2022 The Authors. Published by Elsevier B.V. This is an open access article under the CC BY-NC-ND license (<http://creativecommons.org/licenses/by-nc-nd/4.0/>).

(PPAR $\gamma$ ), a nuclear receptor that is specifically expressed in adipocytes, plays an important role in insulin sensitivity [9]. Activated PPAR $\gamma$  facilitates adipocyte differentiation and increases the number of mature adipocytes with a high insulin sensitivity. The endogenous ligand 15-deoxy- $\Delta^{12,14}$ -prostaglandin J<sub>2</sub> binds to PPAR $\gamma$  and increases the expression of GLUT4 [10]. The PPAR $\gamma$  agonist, rosiglitazone (RSG), a potent antidiabetic agent of thiazolidinediones, accelerates adipocyte differentiation and glucose uptake. In addition, this agonist decreases the number of hypertrophic adipocytes by inducing apoptosis of the adipocytes and consequently increases the number of mature adipocytes [11].

Hormone replacement therapy (HRT) is used to treat climacteric disorders. In this therapy, supplementation with small amounts of estrogen improves glucose metabolism; however, habitual estrogen treatment induces hyperglycemia and insulin resistance. Kami-shoyo-san (KS) is the most frequently used Kampo medicine (traditional Japanese medicine) for climacteric disorders with neurosis, such as irritation, anxiety, and insomnia. Recent studies have shown that KS prolongs the sleep duration of benzodiazepines in ovariectomized mice [12], and is effective in reducing aggressive biting behavior in mice [13]. Moreover, KS promotes estrogen-dependent proliferation of rat pituitary tumor cell lines [14], and postmenopausal women who receive KS with Toki-shakuyaku-san experience raised serum estradiol levels [15].

Paeoniflorin (PF), a monoterpene glucoside, is a bioactive constituent in *Paeonia lactiflora* which is formulated into Kampo medicines with the intent to act as an analgesic and antispasmodic reagent. In recent decades, there has been an increase in the number of reports available on the pharmacology effects of PF. PF is appreciated as a low toxicity, high efficiency, and safety compound, and possesses a variety of pharmacological activities such as anti-inflammatory and immunosuppressive [16], neuroprotective [17], hepatoprotective [18], antitumor [19] activities.

Here, we identified a mechanism by which KS promotes glucose uptake into adipocytes differentiated from 3T3-L1 cells. Furthermore, to elucidate the involvement of PF, a constituent of Kami-shoyo-san, in insulin resistance-associated menopausal pathophysiology, we investigated whether PF suppresses the increase in blood glucose levels caused by estradiol deficiency by increasing estradiol secretion from adipocytes in ovariectomized mice used to simulate menopausal women.

## 2. Materials and methods

### 2.1. Chemicals and reagents

Paeoniflorin (purity  $\geq 97\%$ ) was purchased from the Tokyo Chemical Industry Co., Ltd. (Tokyo, Japan). GW9662 (purity  $\geq 97\%$ ), a PPAR $\gamma$  antagonist, was obtained from Wako Pure Chemical Industries Ltd. (Tokyo, Japan). Dulbecco's modified Eagle's medium-low glucose (DMEM; Merck KGaA, Darmstadt, Germany), fetal bovine serum (FBS; Thermo Fisher Scientific K.K., Tokyo, Japan), isobutyl-methylxanthine (IBMX; FUJIFILM Wako Pure Chemical Corporation), dexamethasone (DEX; Wako Pure Chemical Industries, Ltd.), insulin (FUJIFILM Wako Pure Chemical Corporation), and antibiotic-antimycotic mixed stock solution (100 IU/mL penicillin and 25  $\mu$ g/mL amphotericin B, AB/AM; Nacalai Tesque, Inc., Kyoto, Japan.) was used for cell culture.

### 2.2. Preparation of KS, PR, and KS-PR extraction

Medical-grade Atractylodes Rhizome, Bupleurum Root, Ginger, Glycyrrhiza, Japanese Angelica Root, Jujube, Mentha Herb, Moutan Bark, Paeony Root, and Poria Sclerotium were purchased from Tochimoto Tenkaidou Co., Ltd. (Osaka, Japan). Kami-shoyo-san (KS, prescribed with Atractylodes Rhizome (3.0 g), Bupleurum Root (3.0 g), Ginger (1.0 g), Glycyrrhiza (1.5 g), Japanese Angelica Root (3.0 g), Jujube (2.0 g), Mentha Herb (1.0 g), Moutan Bark (2.0 g), Paeony Root (3.0 g), Poria Sclerotium (3.0 g); Paeony Root (PR, prescribed with

Paeony Root (3.0 g); Kami-shoyo-san excluding Paeony Root (KS-PR); were boiled in 500 mL distilled water until the final volume was reduced by half. After filtration of the obtained decoctions, each filtrate was concentrated under reduced pressure and  $<60^\circ\text{C}$ , and then freeze-dried to obtain the extract.

The amount of KS extract was  $4.76 \pm 0.097507$  mg ( $n = 3$ ), and the KS-PR extract was  $4.37 \pm 0.104559$  mg ( $n = 3$ ). Since the yield of KS-PR extract was 0.918-fold greater than that of KS, the experimental concentration of KS-PR was within the range of 0.918–0.0000918 mg/mL.

### 2.3. 3T3-L1 cell culture

The 3T3-L1 cells were purchased from the Japanese Collection of Research Bioresources Cell Bank (National Institutes of Biomedical Innovation, Health and Nutrition, Osaka, Japan) and cultured  $3 \times 10^4$  cells per well in a 24-well plate at  $37^\circ\text{C}$  and 5% CO<sub>2</sub> for 2 d (day 0–day 2) in the maintenance medium, which contains 10% FBS and 1% AB/AM in DMEM. After reaching confluence, the cells were incubated for 48 h (day 2–day 4) in differentiation induction medium (maintenance medium + 0.5 mM IBMX and 1  $\mu$ M DEX) to differentiate. The medium was replaced with differentiation medium (differentiation induction medium + 1.7  $\mu$ M insulin) and the cells were incubated for 48 h (day 4–day 6). The medium was replaced every 2 d (day 6–day 10) with the maintenance medium in which the sample was dissolved. KS and PR were dissolved in differentiation medium in a 10-fold dilution series covering a range of 1–0.001 mg/mL; KS-PR, 0.918–0.0000918 mg/mL; and paeoniflorin (PF), a PPAR $\gamma$  agonist RSG, a PPAR $\gamma$  antagonist GW9662 (40–0.002 nM). RSG and GW9662 were dissolved in 100% dimethyl sulfoxide (DMSO) and diluted with differentiation medium to the reactive concentrations (40–0.002 nM); the final concentration of DMSO in the medium was 0.15–0.000075% because the cell viability greatly exceeded 120% because of 0.3% DMSO in the media. Four days later (day 10), the medium in each well was collected into a tube, and the cells were used for *Oil-Red-O (ORO) staining* or *glucose uptake assay*. The collected media were stored at  $-80^\circ\text{C}$  until use for *measurement of adiponectin* or *estradiol concentrations*.

### 2.4. 3T3-L1 cytotoxicity assay

Dose-dependent cytotoxicity with KS, PR, KS-PR, PF, and RSG was assessed using the WST-8 [2-(2-methoxy-4-nitrophenyl)-3-(4-nitrophenyl)-5-(2,4-disulfophenyl)-2H-tetrazolium, monosodium salt] with Cell Count Reagent SF (Nakarai Tesque, INC) as follows: 100  $\mu$ L of the 3T3-L1 suspension adjusted  $5 \times 10^3$  cells in maintenance medium was pre-incubated in each well of 96-well plate for 24 h and 5% CO<sub>2</sub> and  $37^\circ\text{C}$  conditioning. Ten microliters of sample solutions prepared using DMEM in an almost 10-fold dilution series covering a range of 2–0.00001 mg/mL (KS and PR), 1.836–0.0000918 mg/mL (KS-PR), and 40 nM–0.002 nM (PF and RSG) were added to each well, and the plate was incubated for 48 h. After addition of 10  $\mu$ L of WST-8 (Cell Count Reagent SF) to each well, the plate was incubated for 2 h. Reduced WST-8 under the electron mediator in the surviving cells was converted to orange-colored formazan. The absorbance of each well was measured at 450 nm wavelength using a spectrophotometric microplate reader (Immuno Mini NJ-2300, Biotech Ltd., Tokyo, Japan). Cell viability (%) was calculated using the following formula:  $(A-B)/(C-B) \times 100$ ; A, absorbance of the sample well; B, blank well (no cells); C, control.

### 2.5. ORO staining

After the 3T3-L1 cell culture step, the 3T3-L1 adipocytes were washed with D-PBS (–) and immobilized with 10% formaldehyde for 1 h at room temperature (around  $20^\circ\text{C}$ ). After incubation with 2-propanol for 1 min, lipid droplets in the cells were stained with ORO (3 mg/mL of 60 (v/v) 2-propanol solution) for 20 min at room temperature (around  $20^\circ\text{C}$ ). Washing with 60% (v/v) 2-propanol, 4% Triton X-100/2-propanol

solution was used to extract ORO in lipid droplets of the adipocytes and measured absorbance of the solutions at 492 nm using a microplate reader (Immuno Mini NJ-2300, BIOTEC Co., Ltd, Tokyo, Japan). Lipid accumulation in adipocytes was quantified using an ORO standard curve in a double dilution series, covering a range of 100–1.5627  $\mu\text{g}/\text{mL}$ . A 4% Triton X-100/2-propanol solution was the zero standard.

## 2.6. Glucose uptake assay

After the *3T3-L1 cell culture* step, the adipocytes were washed once with D-PBS (–) and incubated in the maintenance medium at 37 °C for 1 h or 4 h. The medium was collected and centrifuged at 10,000 rpm for 5 min at 4 °C. The supernatant was stored at –80 °C until use. The glucose concentration in the stored supernatant was measured at 540 nm using a glucose assay kit (Cell Biolabs, Inc., CA, USA) and a microplate reader. Glucose concentration was quantified using a standard curve.

## 2.7. PPAR $\gamma$ binding assay

The PPAR- $\gamma$  binding assay was performed using the method described by Konno et al. [9]. Briefly, cAMP response element binding protein (CRBP)-binding protein (CBP; Bioss Antibodies, Woburn, MA, USA) was immobilized in the plastic wells for 1 h at 37 °C. PPAR $\gamma$  (ProSpec - Tany Techno Gene Ltd., Ness-Ziona, Israel) was immobilized for 24 h at 4 °C after immobilizing 3% skim milk for 1 h at 37 °C as a blocking reagent. Sample solution, PPAR $\gamma$  antibody (rabbit polyclonal; Bio-Rad, Hercules, CA, USA), and IgG antibody conjugated alkaline phosphatase (goat anti-rabbit; Bio-Rad) were added to individual wells and immobilized for 1 h at 37 °C. Para-nitrophenyl phosphate (SIGMAFAST™, Sigma-Aldrich, St Louis, MO, USA) was used as the substrate for alkaline phosphatase. After the development process (shaking at 700 rpm in the dark), the absorbance of each well was measured at 405 nm wavelength. When the absorbance of the sample well was greater than that of the control well, the sample was deemed an agonist of PPAR $\gamma$ . The sample was dissolved in DMSO to prepare a sample solution.

## 2.8. Animals

Nine-week-old female SPF/ICR mice were purchased from Japan SLC, Inc. (Shizuoka, Japan) and housed and maintained under standardized conditions of temperature ( $25 \pm 1$  °C) and humidity ( $55 \pm 5\%$ ) in a light cycle room (light from 07:00 a.m. to 07:00 p.m.; dark from 07:00 p.m. to 07:00 a.m.). The mice were allowed to acclimatize for a week and fed a standard chow (CE-2; CLEA Japan, Inc., Tokyo, Japan).

## 2.9. Ovariectomy and administration procedures

Female 10-week-old ICR mice were ovariectomized under isoflurane anesthesia controlled by inhalation anesthesia systems for rodents (NARCOBIT-E, Natsume Seisakusho, Co., Ltd., Tokyo, Japan). After surgery, lidocaine solution (0.3 mg/mL of 0.9 w/v%) was subcutaneously injected at 3 mg/kg for pain relief with gentamicin ointment (10 mg/kg) to prevent infection of the wound. Lidocaine and gentamicin were administered once daily for 3 d. Seventeen days later, the ovariectomized mice were randomly divided into three groups: control, PF 1 mg/kg, and PF 10 mg/kg, and then ear-punched to distinguish individual mice. A dose of PF was decided by referring to current research focused on the treatment of T2D with PF [20–22]. Subcutaneous injections of the sample were started on the mice once daily for 19 d.

## 2.10. Measurement of estradiol and adiponectin levels

After the *3T3-L1 cell culture* step, adiponectin and estradiol levels in the medium and mouse plasma were determined using enzyme-linked immunosorbent assay (ELISA) kits (Mouse adiponectin/Acrp30 DuoSet® ELISA, DuoSet® ELISA Ancillary Kit 2, Estradiol Parameter Assay

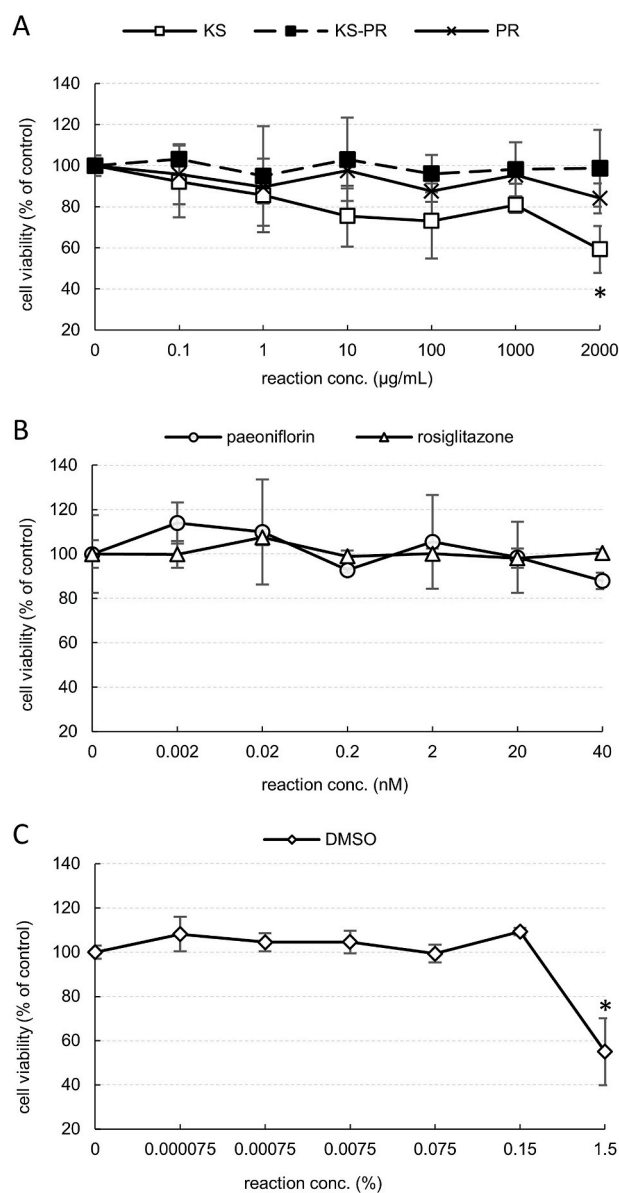


**Fig. 1.** Influences on 3T3-L1 cell viability. **A**, cells treated with KS, PR, or KS-PR (0.1–2000  $\mu\text{g}/\text{mL}$ ); **B**, cells treated with PF or RSG (0.002–40 nM); **C**, cells treated with DMSO (0.000075–0.15 v/v % in the culture medium). All values are presented as the mean  $\pm$  SD ( $n = 4$ ). Statistical analysis was performed using one way ANOVA with multiple comparison procedures performed using Dunnett's test. \*,  $p < 0.05$  vs control. The cells treated with 2000  $\mu\text{g}/\text{mL}$  KS and 1.5% DMSO showed significant decrease in cell viabilities.

Kit, R&D systems, Inc., MN, USA). After the *Ovariectomy and administration procedures* steps, half of the mice in each group were euthanized by inhalation of isoflurane on day 20, and heart blood was immediately collected using a heparin-treated syringe. The blood was centrifuged at 4 °C and 4000 rpm for 15 min to obtain plasma, which was stored in a freezer at –80 °C. The plasma levels of adiponectin and estradiol were determined using an ELISA kit.

## 2.11. Glucose tolerance test of ovariectomized mice

After the *ovariectomy and administration procedures* step, the other half of the mice in each group were assessed using a glucose tolerance test. The mice were fasted for 15 h, and their fasting glucose levels in the tail vein were measured using a blood glucose meter (ACCU-CHEK®A-viva, Roche Diagnostics Co., Ltd., Tokyo, Japan) and a blood glucose test

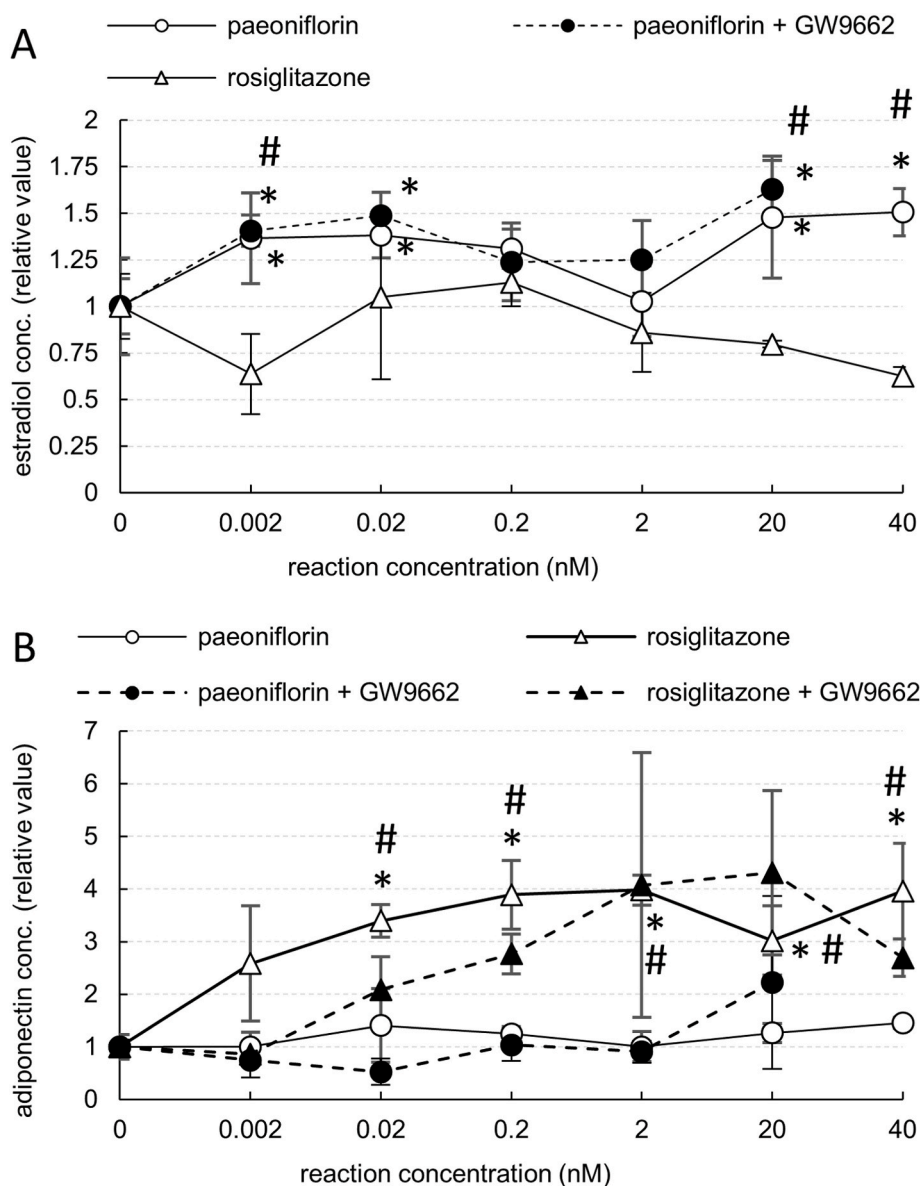


**Fig. 2.** Effects of PF and RSG on estradiol and adiponectin secretions from 3T3-L1 adipocytes. Data are presented as means  $\pm$  SD ( $n = 4$ ). Statistical analysis was performed using one way ANOVA with multiple comparison procedures performed using Dunnett's test (\*,  $p < 0.05$  vs control) or Bonferroni's test (#,  $p < 0.05$ ). **A**, Estradiol level in the culture medium mixed with PF, RSG, or PPAR $\gamma$  inhibitor GW9662 with PF; 3T3-L1 adipocytes treated with 0.002, 0.02, 20, or 40 nM PF significantly increased estradiol secretions compared with control (\* $p < 0.05$ ); the cells treated with 0.002, 0.02, or 20 nM PF + GW9662 showed significant increased estradiol levels compared with control (\* $p < 0.05$ ); the secretion levels from the cells treated with RSG showed significant differences from that of PF at 0.002, 20, or 40 nM (# $p < 0.05$ ). **B**, Adiponectin level in the culture medium mixed with PF, RSG, or PPAR $\gamma$  inhibitor GW9662+PF; 3T3-L1 adipocytes treated with PF showed no significant increase of adiponectin secretion; the cells treated with 0.02, 0.2, 2, 20, or 40 nM RSG showed significant increases of adiponectin secretion (\* $p < 0.05$ ), and these increases showed significant variations from PF (# $p < 0.05$ ); the secretion levels from the cells treated with RSG + GW9662 showed no significant differences compared with control.

paper (ACCU-CHEK Aviva Strip, Roche Diagnostics Co., Ltd.) according to the glucose dehydrogenase enzyme electrode method. Glucose tolerance was evaluated after intraperitoneal injection of D-glucose (1 g/kg) using a meter and test paper. After the glucose tolerance test was completed, mice were euthanized by excessive inhalation of isoflurane.

### 2.12. Calculations and statistical analysis

All data are expressed as the mean values  $\pm$  standard deviation. Comparisons among the means were performed using the Sigma Stat statistical software ver. 2.03 (SPSS, Inc., CA, USA): one-way ANOVA, followed by Dunnett's test for multiple group comparisons and one-way ANOVA, followed by Bonferroni's test for pairwise group comparisons. Statistical significance was set at  $P < 0.05$ .

## 3. Result

### 3.1. Cytotoxic evaluation of 3T3-L1 adipocytes

We performed an WST-8-based assay to evaluate the cytotoxicity of the test samples on 3T3-L1 adipocytes. KS decreased the viability of 3T3-

L1 adipocytes in a concentration-dependent manner, and 2000 mg/mL induced approximately 40% significant decrease in the number of the cells compared to the control (Fig. 1A). Therefore, the reaction concentration of KS used was a 10-fold dilution series covering a range of 1000–0.1  $\mu\text{g/mL}$  in further experimentation. PF showed no cytotoxicity at reaction concentrations ranging from 0.002 to 40 nM (Fig. 1B).

Furthermore, we investigated the cytotoxicity of DMSO, which must be used for RSG dissolution in the culture medium. Based on the results in Fig. 1C, DMSO was determined less than or equal to 0.15% in culture medium. As a result (Fig. 1B), RSG showed no cytotoxicity ranging in the reaction concentrations from 0.002 to 40 nM (DMSO content rate was equivalent to 0.15–0.000075%).

### 3.2. Influence of PF on estradiol and adiponectin secretion of 3T3-L1 adipocytes

As shown in Fig. 2A, estradiol concentrations in the medium used to incubate 3T3-L1 adipocytes were significantly increased by PF at low reaction concentrations (0.002 and 0.02 nM) and at high concentrations (20 and 40 nM). Even when PF was cotreated with GW9662 (PPAR $\gamma$  antagonist) in the medium, the estradiol levels remained high and

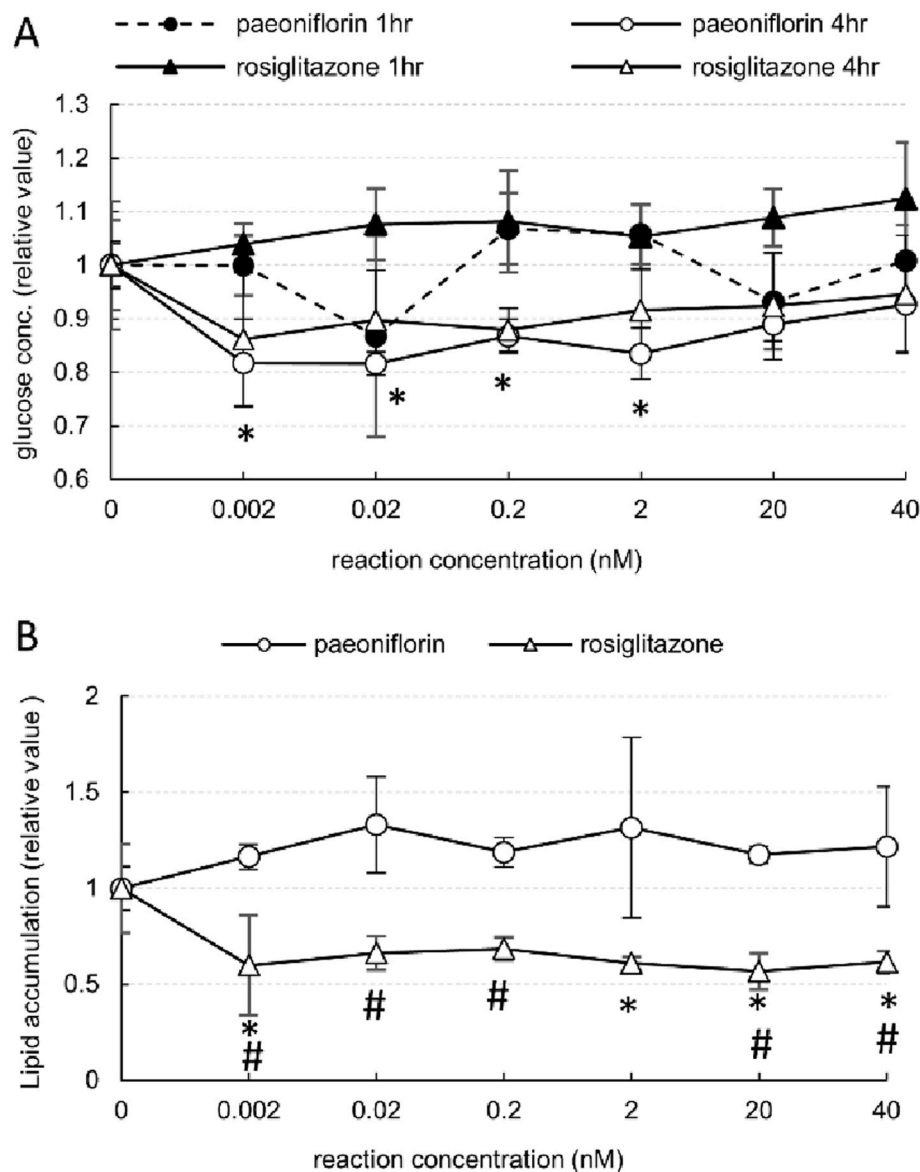


**Fig. 3.** Influences of PF and RSG on glucose uptake and lipid accumulation in 3T3-L1 adipocytes. Data are presented as means  $\pm$  standard deviations ( $n = 4$ ). Statistical analysis was performed using one way ANOVA with multiple comparison procedures performed using Dunnett's test (\*,  $p < 0.05$  vs control) or Bonferroni's test (#,  $p < 0.05$ ). **A**, Glucose level in the culture medium treated with PF or RSG in 1 or 4 h; the cultured medium treated with 0.002, 0.02, 0.2, or 2 nM PF for 4 h showed significant decreases in glucose concentration (\* $p < 0.05$ ). **B**, Lipid accumulation level in 3T3-L1 adipocytes evaluated using ORO staining; the cells treated with 0.002, 2, 20, or 40 nM RSG showed significant reductions of lipid accumulation (\* $p < 0.05$ ); the accumulation levels of PF showed significant differences from that of RSG at 0.002, 0.02, 0.2, 20, or 40 nM (# $p < 0.05$ ).

significantly increased. In contrast, estradiol concentration in the medium was not increased by RSG, a PPAR $\gamma$  agonist. Furthermore, these concentrations were significantly lower than those of PF at high concentrations (20 and 40 nM). It is hypothesized that the PPAR $\gamma$  agonist inhibits estradiol biosynthesis through inhibiting aromatase, which is the rate-limiting enzyme that converts androgen to estradiol, whereas PF has no or limited aromatase inhibitory activity.

As shown in Fig. 2B, adiponectin concentrations in the medium were not increased by PF. Conversely, RSG increased adiponectin concentrations in a concentration-dependent manner, and these concentrations were suppressed by co-treatment with GW9662, a PPAR $\gamma$  antagonist. Thus, PF does not perform as a PPAR $\gamma$  agonist on adipocytes, and it is considered that increased estradiol is negatively correlated with adiponectin secretion.

### 3.3. Influence of PF on glucose uptake and lipid accumulation in 3T3-L1 adipocytes

3T3-L1 adipocytes were treated with PF or RSG for 5 d, with no visible glucose uptake 1 h after the addition of PF or RSG (Fig. 3A). At 4 h after the addition, PF showed a significant concentration-dependent

decrease in glucose concentration in the medium, whereas RSG showed a tendency to decrease the concentration. Therefore, PF robustly promoted glucose uptake into adipocytes.

Glucose is converted to energy through its metabolic pathway; however, surplus glucose is deposited as lipid droplets in adipocytes. The lipid droplets in 3T3-L1 adipocytes were stained red with ORO to evaluate lipid accumulation. As shown in Fig. 3B, RSG significantly reduced lipid accumulation compared to that in the control, and PF showed a tendency to increase lipid accumulation. Thus, PF does not perform as a PPAR $\gamma$  agonist, which facilitates adipocyte apoptosis and differentiation to maintain homeostasis.

### 3.4. Influence of KS on estradiol and adiponectin secretion from 3T3-L1 adipocytes

As shown in Fig. 4A, estradiol levels in culture medium of 3T3-L1 adipocytes were significantly increased by KS at a low concentration (0.0001 mg/mL) and at high concentrations (0.1 and 1 mg/mL), whereas KS-PR showed significantly lower levels than KS at high concentrations. PR significantly increased estradiol concentration in the medium at 0.0001 and 1 mg/mL. These results suggest that PR, a

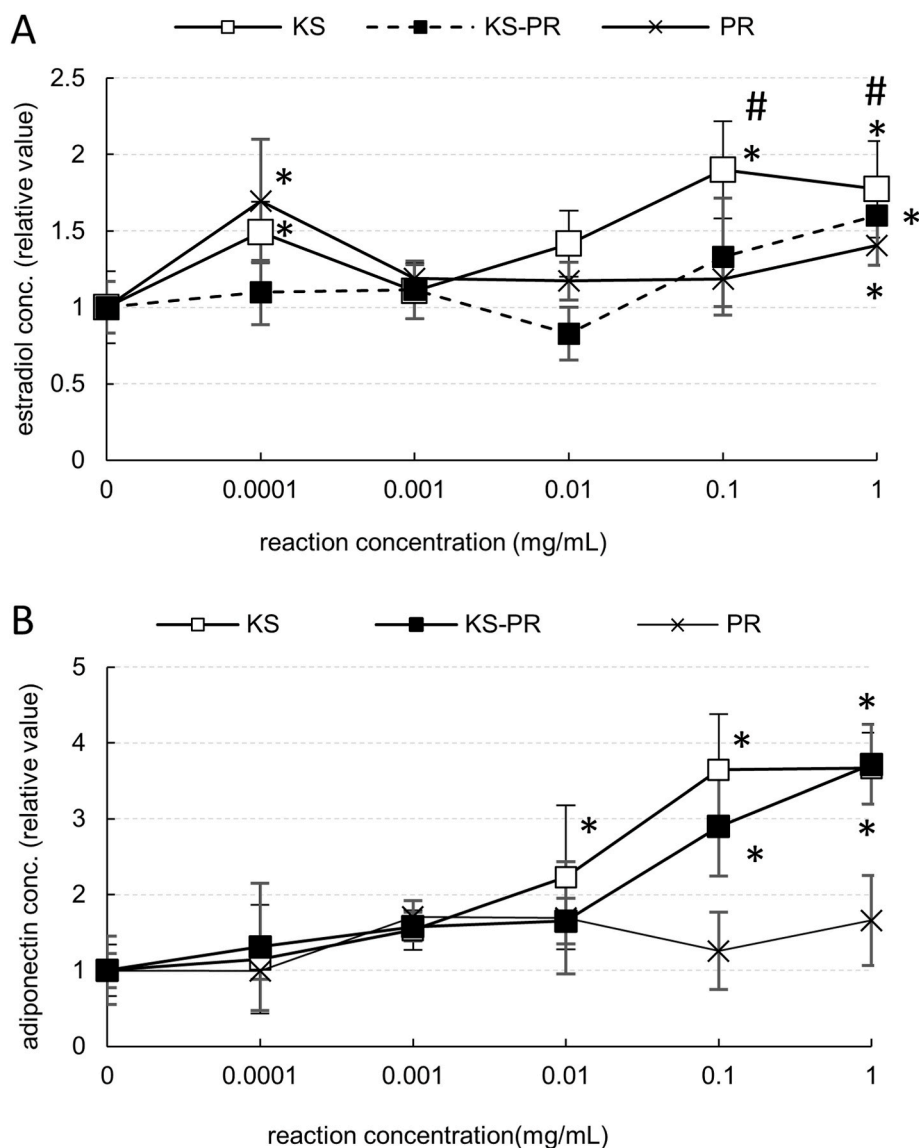


**Fig. 4.** Effects of KS, KS-PR, and PR on estradiol and adiponectin secretions from 3T3-L1 adipocytes. Data are presented as means  $\pm$  standard deviations ( $n = 4$ ). Statistical analysis was performed using one way ANOVA with multiple comparison procedures performed using Dunnett's test (\*,  $p < 0.05$  vs control) or Bonferroni's test (#,  $p < 0.05$ ). **A.** Estradiol level in the culture medium mixed with KS, KS-PR, or PR; 3T3-L1 adipocytes treated with 0.0001, 0.1, or 1 mg/mL KS showed significant increases in estradiol secretion (\* $p < 0.05$ ); the cells treated with 1 mg/mL KS-PR or PR showed significant increases in the secretion (\* $p < 0.05$ ). The estradiol concentrations of KS showed significant decreases compared to those of KS-PR at 0.1 and 1 mg/mL (# $p < 0.05$ ). **B.** Adiponectin level in the medium mixed with KS, KS-PR, or PR; 3T3-L1 adipocytes treated with 0.01, 0.1, or 1 mg/mL KS significantly increased adiponectin secretions (\* $p < 0.05$ ); the adipocytes treated with 0.1 or 1 mg/mL KS-PR showed a significant increase of adiponectin concentration (\* $p < 0.05$ ); PR showed no significant difference of adiponectin level compared with control.

constituent of KS, promotes estradiol secretion from adipocytes.

The adiponectin levels were significantly increased by KS and KS-PR in a concentration-dependent manner (Fig. 4B). No significant differences were observed between the PR and control groups. This suggests that all KS components except PR promote adiponectin secretion from adipocytes.

### 3.5. Influence of KS on glucose uptake and lipid accumulation in 3T3-L1 adipocytes

To evaluate the effect of KS on the glucose uptake system, we measured glucose concentration in the medium used to incubate 3T3-L1 adipocytes treated with KS, KS-PR, or PR. Four hours after the addition of KS, KS-PR, or PR. KS significantly decreased glucose concentration at a high concentration (1 mg/mL), whereas KS-PR and PR showed a decreasing trend (Fig. 5A). Therefore, it is hypothesized that KS promotes glucose uptake into the adipocytes.

Lipid droplets in adipocytes were stained red using ORO to evaluate lipid accumulation. As shown in Fig. 5B, KS and PF significantly increased lipid accumulation in a concentration-dependent manner, whereas KS-PR significantly suppressed lipid accumulation compared to KS at 0.001 and 0.01 mg/mL. These results indicate that PR, a

constituent of KS, promotes lipid accumulation in adipocytes.

### 3.6. Influence of constituents of KS on PPAR $\gamma$ ligand activities

Activation of PPAR $\gamma$  by the agonist is closely related to increased adiponectin secretion from adipocytes. The constituents of KS were examined for their PPAR $\gamma$  ligand activities because KS showed increased adiponectin secretion from 3T3-L1 adipocytes in the present study. Bupleurum root exhibited the highest activity among the crude drugs (Fig. 6A), whereas Glycyrrhiza and Mentha Herb had no activity in the reaction concentration range 0.003–30  $\mu$ g/mL (Fig. 6B). Other constituents of KS exhibited a modest effect on PPAR $\gamma$ ; for instance, Moutan bark and PR, which contain paeoniflorin as the main component, were modestly activated toward PPAR $\gamma$  (Fig. 6A).

### 3.7. Influence of PF on PPAR $\gamma$ ligand activity

PF, a major component of PR, was evaluated for PPAR $\gamma$  ligand activity and PPAR $\gamma$ -competitive inhibition by GW9662, a PPAR $\gamma$  antagonist. As shown in Fig. 7, PF showed PPAR $\gamma$  ligand activities, which were significantly suppressed by equal reaction concentrations of GW9662 at 0.0005 and 0.5  $\mu$ M.

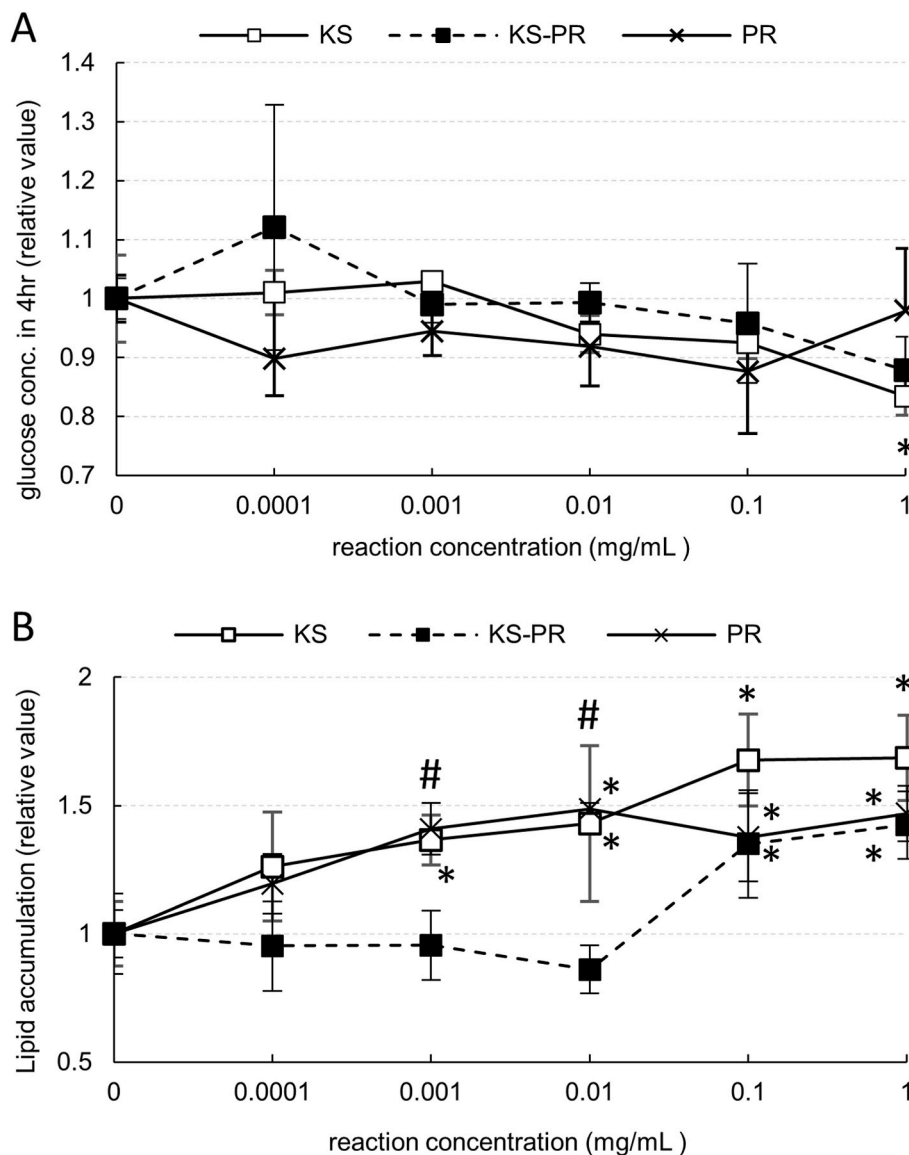


**Fig. 5.** Influences of KS, KS-PR, and PR on glucose uptake and lipid accumulation in 3T3-L1 adipocytes. Data are presented as means ± standard deviations ( $n = 4$ ). Statistical analysis was performed using one way ANOVA with multiple comparison procedures performed using Dunnett's test (\*,  $p < 0.05$  vs control) or Bonferroni's test (#,  $p < 0.05$ ). **A**, Glucose level in the culture medium treated with KS, KS-PR, or PR for 4 h; 3T3-L1 adipocytes cultured with 1 mg/mL KS showed a significant decrease of glucose concentration (\* $p < 0.05$ ). **B**, Lipid accumulation level in 3T3-L1 adipocytes evaluated using ORO staining; the cells treated with 0.001, 0.01, 0.1, or 1 mg/mL KS showed significant increase in lipid accumulation (\* $p < 0.05$ ); 0.1 and 1 mg/mL KS-PR significantly increased the lipids accumulation at 0.1 or 1 mg/mL (\* $p < 0.05$ ); PR showed significant increases of the accumulation at 0.01, 0.1, or 1 mg/mL. The accumulation levels of KS-PR showed significant differences from that of KS at 0.001 and 0.01 mg/mL (# $p < 0.05$ ).

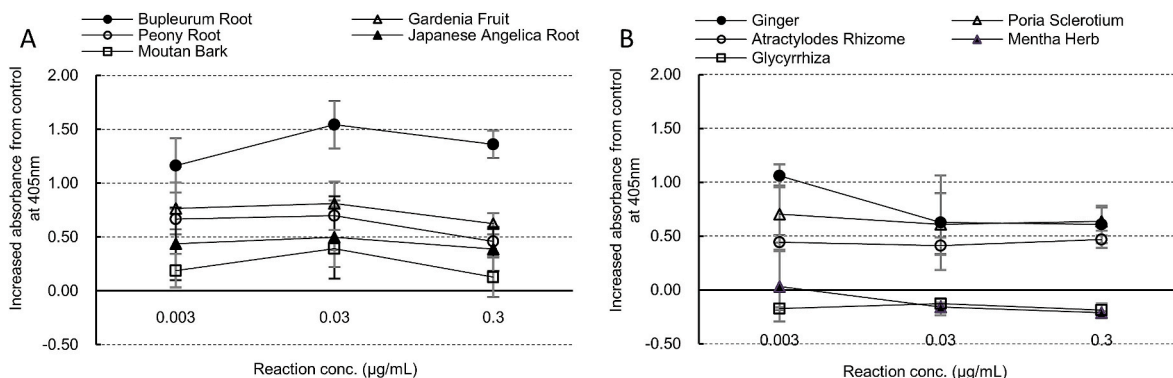


**Fig. 6.** Influences of crude drugs prescribed in KS on PPAR $\gamma$  binding activities. Levels of crude drug-PPAR $\gamma$  binding affinity are proportional to absorbance detected at 405 nm. Data are presented as means ± SD ( $n = 5$ ). **A**, Bupleurum root showed the highest PPAR $\gamma$  binding activity with a peak at 0.03  $\mu\text{g/mL}$ ; gardenia fruit, peony root, Japanese Angelica root, and Moutan bark moderately increased the absorbance with a peak at 0.03  $\mu\text{g/mL}$ . **B**, Ginger, Poria sclerotium, and Atractylodes rhizome showed no concentration-dependent PPAR $\gamma$  binding activity, and Mentha herb and glycyrrhiza showed no activity.

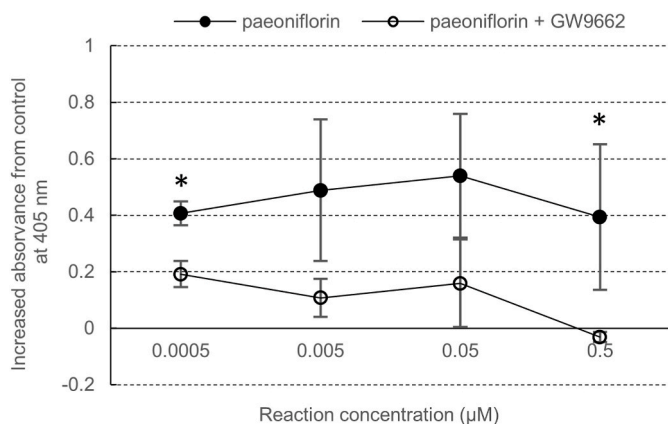


**Fig. 7.** PPAR $\gamma$  binding activities of PF. Data are presented as means  $\pm$  SD ( $n = 3$ ). Statistical analysis was performed using Student's  $t$ -test (\*,  $p < 0.05$ ). Increased PPAR $\gamma$  binding activities of PF were significantly inhibited by adding GW9662 at 0.0005 and 0.5  $\mu\text{M}$ .

### 3.8. Influence of PF on blood estradiol and adiponectin levels

To investigate the effect of PF in a mouse model of climacteric disorder, PF was subcutaneously injected into ovariectomized mice without sex hormone treatment and adipocyte-released hormones in the blood were measured. PF-treated mice showed a trend toward increased blood estradiol levels in a dose-dependent manner (Fig. 8A), whereas the mice showed significantly decreased blood adiponectin levels in a concentration-dependent manner (Fig. 8B). These findings suggest that adipocytes treated with PF may promote estradiol secretion instead of the ovary, and increased estradiol secretion is negatively correlated with adiponectin secretion.

### 3.9. Influence of PF on blood glucose levels

Estradiol has been reported to correlate with abnormal glucose tolerance [4]. Therefore, the glucose tolerance test (GTT) was performed to investigate whether PF suppresses elevated blood glucose levels in ovariectomized mice. PF (10 mg/kg) significantly suppressed blood glucose levels before D-glucose loading (0 min) and 30 min after loading (Fig. 9), indicating that PF has the potential to improve impaired blood glucose levels and postprandial hyperglycemia caused by estradiol

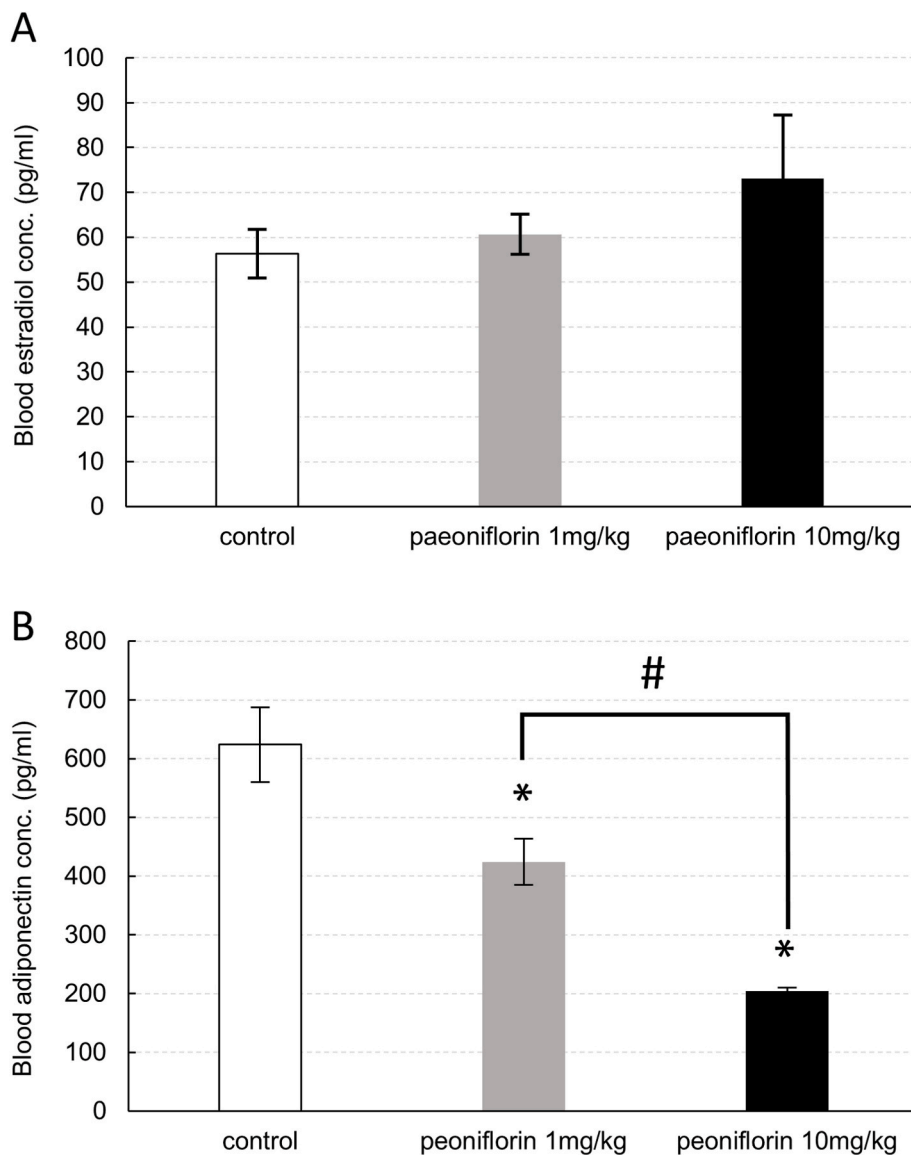


**Fig. 8.** Effects of PF on blood estradiol and adiponectin levels in ovariectomized mice. Data are presented as means  $\pm$  SD ( $n = 5$ ). Statistical analysis was performed using one way ANOVA with multiple comparison procedures performed using Dunnett's test (\*,  $p < 0.05$  vs control) or Bonferroni's test (#,  $p < 0.05$ ). **A**, PF showed a trend toward increased blood estradiol levels in a dose-dependent manner. **B**, Blood adiponectin levels in mice treated with 1 or 10 mg/kg PF were significantly decreased compared with the control (\*,  $p < 0.05$ ); #, significant difference between the groups of 1 and 10 mg/kg PF.

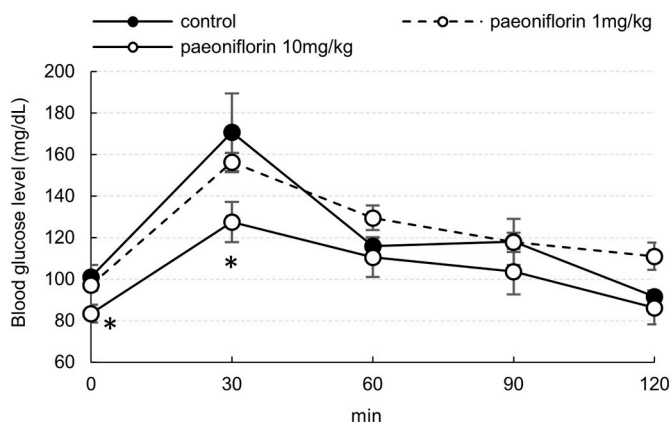


**Fig. 9.** Glucose tolerance test of ovariectomized mice treated with PF. Data are presented as means  $\pm$  SD ( $n = 5$ ). Statistical analysis was performed using one way ANOVA with multiple comparison procedures performed using Dunnett's test (\*,  $p < 0.05$  vs control). Time-dependent changes in blood glucose levels were measured after intraperitoneal injection of 1 g/kg D-glucose; in the 10 mg/kg PF-treated group, 0 and 30 min of blood glucose levels were significantly suppressed compared with that of the control group.

deficiency.

#### 4. Discussion

In female climacteric disorders, adipose tissue is an important site of estradiol biosynthesis by aromatase (gene name: *CYP19A1*), which is the rate-limiting enzyme that is induced during adipogenesis and the adipocyte differentiation process [23]. Estradiol bound to ESR1 stimulates glucose uptake into adipocytes through the intranuclear and extranuclear pathways: (1) GLUT4 protein synthesis and (2) AKT phosphorylation in the insulin signaling pathway [6]. In the present study, we found that paeoniflorin (PF) significantly promotes estradiol secretion from 3T3-L1 adipocytes (Fig. 2A) and glucose uptake into

adipocytes (Fig. 3A). Li et al. reported that PF ameliorates insulin resistance by activating AMPK and AKT phosphorylation in the livers of male Sprague-Dawley rats [20]. Furthermore, PF induces the release of adenosine from isolated white adipocytes in Wistar rats to enhance glucose uptake [24]. In both preadipocytes and adipocytes, Cx43 is the major component of the gap junction connecting the cytoplasm of two neighboring cells, and the downregulation of Cx43 results in reduced expression of C/EBP $\beta$  and adipogenesis suppression [25]. Adipogenesis is defined as the process by which fibroblast-like preadipocytes develop into mature adipocytes. It is also reported that 17 $\beta$ -estradiol induces gap junction and Cx43 phosphorylation through the MEK/ERK signaling pathway [26]. Here, we present a novel mechanism through which PF activates AMPK phosphorylation and adipocyte differentiation by increasing estradiol biosynthesis, which leads to glucose uptake (Fig. 10A).

RSG is known to promote adipocyte differentiation into mature, small adipocytes and the apoptosis of large adipocytes, consequently increasing the number of mature adipocytes with high insulin sensitivity. In the present study, RSG showed a trend toward a decrease in estradiol secretion from 3T3-L1 adipocytes (Fig. 2A) and a trend toward increased glucose uptake into 3T3-L1 adipocytes (Fig. 3A). Araki et al. reported that RSG directly inhibited estrogen synthesis in human ovarian cell cultures, and the RSG did not affect aromatase mRNA or protein expression [27]. Furthermore, as shown in Fig. 2B, RSG increased adiponectin secretion from the cells, whereas PF had no influence on secretion. Therefore, PF is considered to decrease blood glucose levels through a route distinct from RSG, as indicated in Fig. 10.

PF, which is the main ingredient of paeony root (PR), has a moderate level of PPAR $\gamma$  binding activity (Fig. 6). Therefore, we hypothesized that PF is likely to inhibit aromatase activity and reduce estradiol synthesis in adipose tissue, similar to the potent inhibitor RSG. In this study, PF showed a gradual decrease in estradiol concentration from 0.02 to 2 nM, indicating that PF may influence estradiol biosynthesis through its PPAR $\gamma$  binding activity. However, the estradiol concentrations were not lower than those of the control, suggesting that PF is not a potent PPAR $\gamma$  activator such as RSG. Moreover, aromatase is known as a rate-limiting

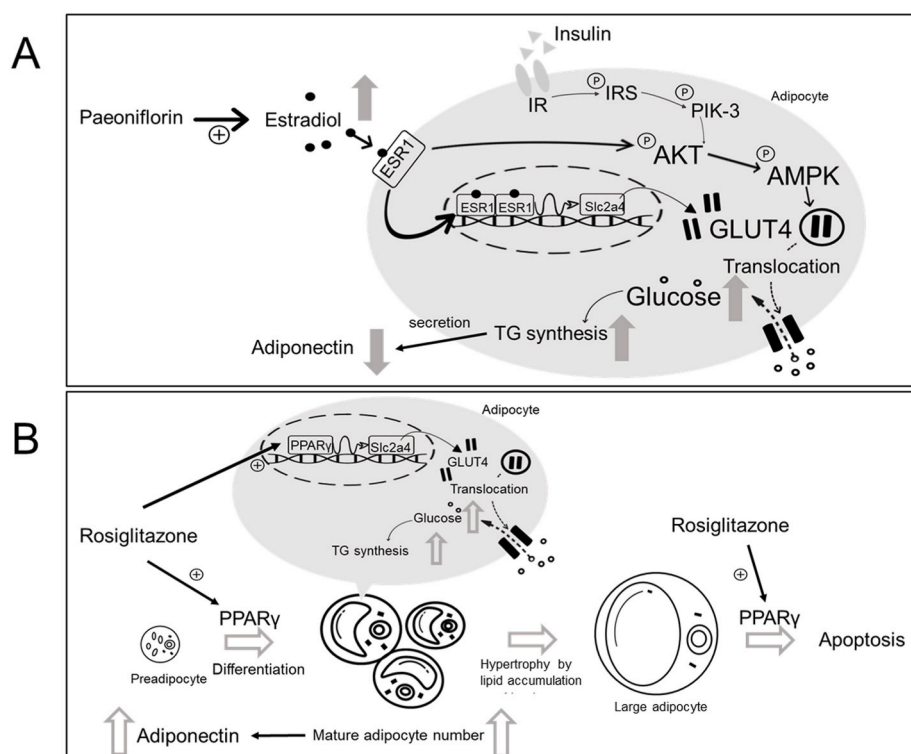


**Fig. 10.** The mechanism of PF and RSG for affecting glucose uptake and adiponectin secretion. **A**, The mechanism by which PF promotes glucose uptake into adipocytes; (1) PF promotes estradiol secretion by stimulating estradiol synthesis; (2) estradiol binds to ESR1 to increase transcription of Scl2a4 encoding GLUT4 and phosphorylation of AKT, thus inducing glucose uptake through GLUT4; (3) adiponectin secretion is reduced by glucose-induced triglyceride accumulation in adipocytes. **B**; The mechanism by which RSG promotes glucose uptake into adipocytes; (1) RSG bound to PPAR $\gamma$  increases transcription of Scl2a4 encoding GLUT4, inducing glucose uptake; (2) activated PPAR $\gamma$  by RSG leads to apoptosis of large adipocytes; (3) the number of mature adipocytes differentiated from pre-adipocyte is increased, leading to an increase in adiponectin secretion from mature adipocytes.

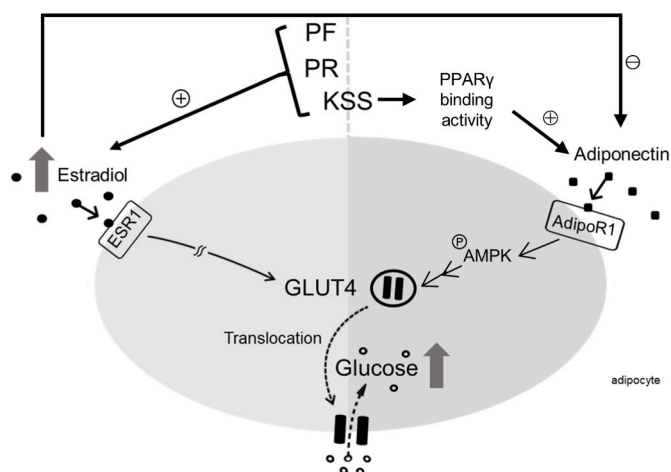


**Fig. 11.** The mechanism of KS for regulating glucose uptake. PF, PR, and KS stimulate glucose uptake by altering estradiol production, leading to GLUT4 translocation; PF shows a reduction of adiponectin production accompanied with an increase of estradiol production. This decrease can be compensated by KS, which increases both estradiol and adiponectin production.

enzyme that can be allosterically modulated with high potency, and may have a role in modulating estradiol synthesis as a regulatory factor on the allosteric site of aromatase.

KS has been reported to be effective in treating climacteric disorders in HRT-resistant patients [28]. As shown in Fig. 4A, KS exhibited increased estradiol secretion, which was significantly attenuated by the exclusion of PR from the KS prescription (KS-PR). It is hypothesized that the increased estradiol secretion by KS was about the result of the constituent crude drug PR in the KS formulation. As shown in Fig. 4B, KS increased adiponectin secretion from 3T3-L1 adipocytes, whereas PR had no effect on adiponectin secretion. Yamauchi et al. demonstrated that the adipocyte-derived hormone adiponectin activates AMPK in the insulin signaling pathway [29], thereby directly increasing glucose uptake. The constituent crude drugs other than PR in the KS formulation are considered to contribute to glucose uptake by increasing adiponectin secretion through PPAR $\gamma$  activation, as indicated in Fig. 11.

We explored the effects of PF on postprandial hyperglycemia and the levels of plasma adipokines (adiponectin and estradiol) in ovariectomized mice, modeled as menopausal women. PF significantly suppressed blood glucose levels in fasting and post-loading glucose in menopausal model mice (Fig. 9) because PF showed a trend toward increased blood estradiol levels in a concentration-dependent manner (Fig. 8A), indicating that the effective suppression of blood glucose levels by PF may be mediated by increased blood estradiol levels. PF caused a concentration-dependent decrease in adiponectin levels in ovariectomized mice (Fig. 8B). Pektaş et al. reported that 17 $\beta$ -estradiol can modify adipokine production in 3T3-L1 adipocytes and decrease adiponectin levels [30]. Blood adiponectin levels are inversely correlated with the number of large adipocytes that store lipid droplets converted from surplus blood glucose. The production of large adipocytes enhances macrophage infiltration and the production of macrophage-derived TNF $\alpha$ , which is known to augment inflammatory changes and insulin resistance [31]. Kong et al. provided important evidence that PF ameliorates TNF $\alpha$ -mediated insulin resistance and inflammatory adipokine release from 3T3-L1 adipocytes by suppressing the activation of IKK/NF- $\kappa$ B and JNK/SAPK, which are involved in the insulin signaling pathway, and enhances PPAR $\gamma$  expression in 3T3-L1 adipocytes, but not PPAR $\gamma$  activation [32]. It has also been reported that increased ER $\alpha$ -bound estradiol levels are associated with a decrease in the production of Arg1, which is related to the pro-inflammatory response [33]. Mitochondria existing in white adipocytes are involved in maintaining metabolic homeostasis, and impaired mitochondrial

function is directly linked to the development of metabolic diseases such as diabetes and insulin resistance. It was reported the existence of ER $\alpha$  in mitochondria, and treatment with 17 $\beta$ -estradiol to 3T3-L1 adipocytes prevented IL6-induced inflammation of the inner mitochondrial membrane and improved the mitochondrial function in the adipocytes [34]. Although increased estradiol secretion by PF can induce a decrease in adiponectin secretion, PF-induced upregulation of estradiol biosynthesis may suppress secretion of pro-inflammatory cytokines (for example, TNF $\alpha$ , IL1 $\beta$ , and IL6) from hypertrophic adipocytes and may inhibit insulin resistance leading to T2D.

Obesity is the most remarkable risk factor for the development of T2D. Digestive enzyme inhibitors have been identified from various natural products for decreasing the absorption of dietary carbohydrates and for preventing obesity [35]. Several pathophysiologic abnormalities, such as estrogen reduction and hemochromatosis, have also been associated with T2D. Hemochromatosis induces insulin resistance caused by the accumulation of excess iron to  $\beta$ -cells in pancreas islets [36] and indicates a reduction of the iron regulatory hormone hepcidin or a reduction of hepcidin/ferritin ratio in blood [37]. Menopausal women have abnormal glucose homeostasis that may lead to T2D due to sex hormone deficiency. KS may improve T2D associated with climacteric disorder because its ingredient PF has the potential to suppress blood glucose levels by increasing estradiol secretion from adipose tissue.

## 5. Conclusions

Estradiol deficiency can cause metabolic abnormalities such as insulin resistance, leading to T2D. In the present study, paeoniflorin (PF) promoted estradiol synthesis in 3T3-L1 adipocytes, leading to the stimulation of AKT phosphorylation in the insulin signaling pathway, increased GLUT4 expression, and adipocyte differentiation. PF is obtained from peony root (PR), which is a constituent of Kami-shoyo-san (KS). Our study revealed that KS increases estradiol secretion from adipocytes and promotes glucose uptake. The PPAR $\gamma$  agonist RSG, a therapeutic drug for T2D, showed a trend toward decreased estradiol secretion from 3T3-L1 adipocytes. Therefore, PPAR $\gamma$  antidiabetic agents may have adverse effects on climacteric disorders. Although PF exhibited decreased PPAR $\gamma$  ligand activity, estradiol synthesis was not significantly decreased compared to that of the control. KS increased the secretion of both estradiol and adiponectin in adipocytes. PF used alone for T2D may cause adipocyte hypertrophy because of decreased adiponectin levels in ovariectomized mice; however, KS is expected to reduce the incidence of T2D caused by estradiol deficiency. Furthermore, it is reported that increased estradiol secretion from adipocytes is correlated with the risk of developing breast cancer because estradiol reduces the secretion of adiponectin which has the ability to apoptosis breast cancer cells [38]. In the present report, PF increased the amount of estradiol secretion from adipocytes; instead, PF reduced the secretion amount of adiponectin, which raised concern about the risk of breast cancer. However, PF has also been reported to suppress the differentiation and invasion of breast cancer cells [39] and thus might lower the risk of breast cancer development during menopause which compensatory increases estrogen secretion from adipocytes because of decreased secretion of the ovarian estrogen. We expect to be able to clinically use the compound that simultaneously reduces the risk of developing breast cancer and diabetes in menopausal women.

## Ethical approval of animal experiments

Animal experiments were approved by the Animal Experimental Committee of Tohoku Medical and Pharmaceutical University (approval no. A21027-cn), and the experimental procedures were conducted in accordance with the ethical guidelines of the university.

## Author contributions

Kyoko Kobayashi: Conceptualization, Methodology, Formal analysis, Investigation, Project administration, Visualization, Writing – original draft, Writing – review & editing. Yu Ting Tang: Formal analysis, Investigation, Visualization. Kenroh Sasaki: Supervision, Validation.

## Funding

This research did not receive any specific grant from funding agencies in the public, commercial, or not-for-profit sectors.

## Declaration of competing interest

The authors declare that they have no known competing financial interests or personal relationships that could have appeared to influence the work reported in this paper.

## Acknowledgment

The authors would like to thank Y. Nishikawa and past members of our laboratory for technical assistance with the experiments.

## References

- M. Franck, J. is estradiol a biomarker of type 2 diabetes risk in postmenopausal women? *Diabetes* 66 (2017) 568–570, <https://doi.org/10.2337/dbi16-0063>.
- K.L. Margolis, D.E. Bonds, R.J. Rodabough, L. Tinker, L.S. Phillips, C. Allen, T. Bassford, G. Burke, J. Torrens, B.V. Howard, Effect of oestrogen plus progestin on the incidence of diabetes in postmenopausal women: results from the Women's Health Initiative Hormone Trial, *Diabetologia* 47 (2004) 1175–1187, <https://doi.org/10.1007/s00125-004-1448-x>.
- H. Cui, G. Zhao, J. Wen, W. Tong, Follicle-stimulating hormone promotes the transformation of cholesterol to estrogen in mouse adipose tissue, *Biochem. Biophys. Res. Commun.* 495 (2018) 2331–2337, <https://doi.org/10.1016/j.bbrc.2017.12.120>.
- J.Y. Kim, K.J. Jo, B.J. Kim, H.W. Baik, S.K. Lee, 17 $\beta$ -estradiol induces an interaction between adenosine monophosphate-activated protein kinase and the insulin signaling pathway in 3T3-L1 adipocytes & Estradiol-induced regulation of GLUT4 in 3T3-L1 cells: involvement of ESRI and AKT activation, *Int. J. Mol. Med.* 30 (2012) 979–985, <https://doi.org/10.3892/ijmm.2012.1070>.
- F.S. Camila, L.R.S. Stopa, G.F. Santos, L.C.N. Takasumi, A.B. Martins, M.C. Garnica-Siqueira, R.N. Ferreira, F.G. de Andrade, C.M. Leite, D.A.M. Zaia, C.T.B.V. Zaia, E. T. Uchoa, Estradiol protects against ovariectomy-induced susceptibility to the anabolic effects of glucocorticoids in rats, *Life Sci.* 218 (2019) 185–196, <https://doi.org/10.1016/j.lfs.2018.12.037>.
- R.S. Campello, A. Luciana, L.A. Fátima, J.N. Barreto-Andrade, T.F. Lucas, R. C. Mori, C.S. Porto, U.F. Machado, Estradiol-induced regulation of GLUT4 in 3T3-L1 cells: involvement of ESRI and AKT activation, *J. Mol. Endocrinol.* 59 (2017) 257–268, <https://doi.org/10.1530/JME-17-0041>.
- T.P. Combs, A.H. Berg, M.W. Rajala, S. Klebanov, P. Iyengar, J.C. Jimenez-Chillaron, M.E. Patti, S.L. Klein, R.S. Weinstein, P.E. Scherer, Sexual Differentiation, Pregnancy, Calorie Restriction, Aging Affect, The adipocyte-specific secretory protein adiponectin, *Diabetes* 52 (2003) 268–276, <https://doi.org/10.2337/diabetes.52.2.268>.
- K. Yamada, N. Harada, Expression of estrogen synthetase (P-450 aromatase) during adipose differentiation of 3T3-L1 cells, *Biochem. Biophys. Res. Commun.* 169 (1990) 531–536, [https://doi.org/10.1016/0006-291X\(90\)90363-R](https://doi.org/10.1016/0006-291X(90)90363-R).
- T. Konno, K. Sasaki, K. Kobayashi, T. Murata, Indirubin promotes adipocyte differentiation and reduces lipid accumulation in 3T3 L1 cells via peroxisome proliferator activated receptor  $\gamma$  activation, *Mol. Med. Rep.* 21 (2020) 1552–1560, <https://doi.org/10.3892/mmr.2020.10946>.
- B.M. Forman, P. Tontonoz, J. Chen, R.P. Brun, B.M. Spiegelman, R.M. Evans, 15-deoxy- $\Delta^{12,14}$ -prostaglandin  $J_2$  is a ligand for the adipocyte determination factor PPAR $\gamma$ , *Cell* 83 (1995) 803–812, [https://doi.org/10.1016/0092-8674\(95\)90193-0](https://doi.org/10.1016/0092-8674(95)90193-0).
- T. Yamauchi, J. Kamon, H. Waki, K. Murakami, K. Motojima, K. Kameda, T. Ide, N. Kubota, Y. Terauchi, K. Tobe, H. Miki, A. Tsuchida, Y. Akanuma, R. Nagai, S. Kimura, T. Kadowaki, The mechanisms by which both heterozygous peroxisome proliferator-activated receptor gamma (PPAR gamma) deficiency and PPAR gamma agonist improve insulin resistance, *J. Biol. Chem.* 276 (2001) 41245–41254, <https://doi.org/10.1074/jbc.M103241200>.
- N. Egashira, Y. Goto, H. Iba, R. Kawanaka, R. Takahashi, C. Taniguchi, T. Watanabe, K. Kubota, S. Katsurabayashi, K. Iwasaki, Kamishoyosan potentiates pentobarbital-induced sleep in socially isolated, ovariectomized mice, *J. Ethnopharmacol.* 281 (2021) 114585, <https://doi.org/10.1016/j.jep.2021.114585>.
- J. Igarashi, T. Kuchiiwa, S. Kuchiiwa, H. Iwai, K. Tomita, T. Sato, Kamishoyosan (a Japanese traditional herbal formula), which effectively reduces the aggressive biting behavior of male and female mice, and potential regulation through increase of Tph1, Tph2, and Esr2 mRNA levels, *Brain Res.* 1768 (2021) 147580, <https://doi.org/10.1016/j.brainres.2021.147580>.
- Z. Wang, S. Kanda, T. Shimono, D. Enkh-Undraa, T. Nishiyama, The in vitro estrogenic activity of the crude drugs found in Japanese herbal medicines prescribed for menopausal syndrome was enhanced by combining them, *BMC Compl. Alternative Med.* 18 (2018) 107, <https://doi.org/10.1186/s12906-018-2170-4>.
- B. Pan, Y. Kato, K. Sengoku, N. Takuma, N. Niizeki, M. Shikawa, Treatment of climacteric symptoms with herbal formulas of traditional Chinese medicine, *Gynecol. Obstet. Invest.* 57 (2004) 144–148, <https://doi.org/10.1159/000076003>.
- Y. Zhou, X. Gong, H. Zhang, C. Peng, A review on the pharmacokinetics of paeoniflorin and its anti-inflammatory and immunomodulatory effects, *Biomed. Pharmacother.* 130 (2020) 110505, <https://doi.org/10.1016/j.biopha.2020.110505>.
- J. Li, X. Ji, J. Zhang, G. Shi, X. Zhu, K. Wang, Paeoniflorin attenuates A $\beta$ 25-35-induced neurotoxicity in PC12 cells by preventing mitochondrial dysfunction, *Folia Neuropathol.* 52 (2014) 285–290, <https://doi.org/10.5114/fn.2014.45569>.
- Z. Jiang, W. Chen, X. Yan, L. Bi, S. Guo, Z. Zhan, Paeoniflorin protects cells from GalN/TNF- $\alpha$ -induced apoptosis via ER stress and mitochondria-dependent pathways in human L02 hepatocytes, *Acta Biochim. Biophys. Sin.* 46 (2014) 357–367, <https://doi.org/10.1093/abbs/gmu010>.
- X. Wang, L. Xia, X. Zhang, Q. Chen, X. Li, Y. Mou, T. Wang, Y. Zhang, The multifaceted mechanisms of Paeoniflorin in the treatment of tumors: state-of-the-art, *Biomed. Pharmacother.* 149 (2022) 112800, <https://doi.org/10.1016/j.biopha.2022.112800>.
- Y. Li, J. Qiao, B. Wang, M. Bai, J. Shen, Y. Cheng, Paeoniflorin ameliorates fructose-induced insulin resistance and hepatic steatosis by activating LKB1/AMPK and AKT pathways, *Nutrients* 10 (2018) 1024, <https://doi.org/10.3390/nu10081024>.
- Y. Huang, J. Wang, L. Yang, L. Yue, L. Zhang, Y. Zhang, Y. Song, D. Lid, Z. Yang, Paeoniflorin ameliorates glycemic variability-induced oxidative stress and platelet activation in HUVECs and DM rats, *RSC Adv.* 10 (2020) 42605, <https://doi.org/10.1039/d0ra02036b>.
- J. Wang, Y. Huang, S. Zhang, H. Yin, L. Zhang, Y. Zhang, Y. Song, D. Li, A protective role of paeoniflorin in fluctuant HyperglycemiaInduced vascular endothelial injuries through antioxidative and anti-inflammatory effects and reduction of PKC $\beta$ 1, *Oxid. Med. Cell. Longev.* (2019), 5647219, <https://doi.org/10.1155/2019/5647219>, 11.
- L. Leitner, A. Jürets, B.K. Itariu, M. Keck, G. Prager, F. Langer, V. Greblowitz, M. Zeyda, Osteopontin promotes aromatase expression and estradiol production in human adipocytes, *Breast Cancer Res. Treat.* 154 (2015) 63–69, <https://doi.org/10.1007/s10549-015-3603-0>.
- L.M. Tang, I.M. Liu, J.T. Cheng, Stimulatory effect of paeoniflorin on adenosine release to increase the glucose uptake into white adipocytes of wistar rat, *Planta Med.* 69 (2003) 332–336, <https://doi.org/10.1055/s-2003-38878>.
- T. Yanagiyama, A. Tanabe, K. Hotta, Gap-junctional communication is required for mitotic clonal expansion during adipogenesis, *Obesity* 15 (2007) 572–582, <https://doi.org/10.1038/oby.2007.547>.
- J. Duan, H. Chen, Y. Li, D. Xu, X. Li, Z. Zhang, J. Cheng, L. Yang, Q. Li, 17 $\beta$ -Estradiol enhances porcine meiosis resumption from autophagy-induced gap junction intercellular communications and connexin 43 phosphorylation via the MEK/ERK signaling pathway, *J. Agric. Food Chem.* 69 (2021) 11847–11855, <https://doi.org/10.1021/acs.jafc.1c04212>.
- T. Araki, M. Varadinova, M. Goldman, S. Rosenwaks, L. Poretsky, D. Seto-Young, Rosiglitazone, Pioglitazone Alter, Aromatase kinetic properties in human granulosa cells, *PPAR res*, Article ID 926438 (2011) 5, <https://doi.org/10.1155/2011/926438>.
- T. Hidaka, R. Yonezawa, S. Saito, Kami-shoyo-san, Kampo (Japanese traditional medicine), is effective for climacteric syndrome, especially in hormone-replacement-therapy-resistant patients who strongly complain of psychological symptoms, *J. Obstet. Gynaecol. Res.* 39 (2012) 223–228, <https://doi.org/10.1111/j.1447-0756.2012.01936.x>.
- T. Yamauchi, J. Kamon, Y. Minokoshi, Y. Ito, H. Waki, S. Uchida, S. Yamashita, M. Noda, S. Kita, K. Ueki, K. Eto, Y. Akanuma, P. Froguel, F. Foufelle, P. Ferre, D. Carling, S. Kimura, R. Nagai, B.B. Kahn, T. Kadowaki, Adiponectin stimulates glucose utilization and fatty-acid oxidation by activating AMP-activated protein kinase, *Nat Med* 8 (2002) 1288–1295, <https://doi.org/10.1038/nm788>.
- M. Pektaş, A.H. Kurt, I. Ün, R.N. Tiftik, K. Büyükkafşar, Effects of 17 $\beta$ -estradiol and progesterone on the production of adipokines in differentiating 3T3-L1 adipocytes: role of Rho-kinase, *Cytokine* 72 (2015) 130–134, <https://doi.org/10.1016/j.cyt.2014.12.020>.
- T. Suganami, J. Nishida, Y. Ogawa, A paracrine loop between adipocytes and macrophages aggravates inflammatory changes: role of free fatty acids and tumor necrosis factor alpha, *Arterioscler. Thromb. Vasc. Biol.* 25 (2005) 2062–2068, <https://doi.org/10.1161/01.ATV.0000183883.72263.13>.
- P. Kong, R. Chi, L. Zhang, N. Wang, Y. Lu, Effects of paeoniflorin on tumor necrosis factor- $\alpha$ -induced insulin resistance and changes of adipokines in 3T3-L1 adipocytes, *Fitoterapia* 91 (2013) 44–50, <https://doi.org/10.1016/j.fitote.2013.08.010>.
- A. Villa, N. Rizzi, E. Vegeto, P. Ciana, A. Maggi, Estrogen accelerates the resolution of inflammation in macrophagic cells, *Sci. Rep.* 5 (2015), 15224, <https://doi.org/10.1038/srep15224>, 14.
- M. Bauzá-Thorbürggea, S. Rodríguez-Cuenca, A. Vidal-Puig, B. Galmés-Pascual, M. Sbert-Roig, M. Gianotti, I. Lladó, A. Proenza, GPER and ER $\alpha$  mediate estradiol enhancement of mitochondrial function in inflamed adipocytes through a PKA

- dependent mechanism, *J. Steroid Biochem. Mol. Biol.* 185 (2019) 256–267, <https://doi.org/10.1016/j.jsbmb.2018.09.013>.
- [35] L. Zheng, X. Chen, K. Cheong, Current trends in marine algae polysaccharides: the digestive tract, microbial catabolism, and prebiotic potential, *Int. J. Biol. Macromol.* 151 (2020) 344–354, <https://doi.org/10.1016/j.ijbiomac.2020.02.168>.
- [36] R. Cooksey, H. Jouihan, R. Ajioka, M. Hazel, D. Jones, J. Kushner, D. McClain, Oxidative stress, beta-cell apoptosis, and decreased insulin secretory capacity in mouse models of hemochromatosis, *Endocrinol* 145 (2004) 5305–5312, <https://doi.org/10.1210/en.2004-0392>.
- [37] N. Karamzad, A. Eftekhari, A. Ashrafi-Asgarabad, M. Sullman, A. Sahebkar, S. Safiri, Serum hepcidin, the hepcidin/ferritin ratio and the risk of type 2 diabetes: a systematic review and meta-analysis, *Curr. Med. Chem.* 28 (2021) 1224–1233, <https://doi.org/10.2174/0929867327666200207120158>.
- [38] G. Pfeiler, C. Buechler, M. Neumeier, A. Schäffler, G. Schmitz, O. Ortmann, O. Treeck, Adiponectin effects on human breast cancer cells are dependent on 17-beta estradiol, *Oncol. Rep.* 19 (2008) 787–793, <https://doi.org/10.3892/or.19.3.787>.
- [39] Q. Zhang, Y. Yuan, J. Cui, T. Xiao, D. Jiang, Paeoniflorin inhibits proliferation and invasion of breast cancer cells through suppressing Notch-1 signaling pathway, *Biomed Pharmacothr* 78 (2016) 197–203, <https://doi.org/10.1016/j.biopha.2016.01.019>.